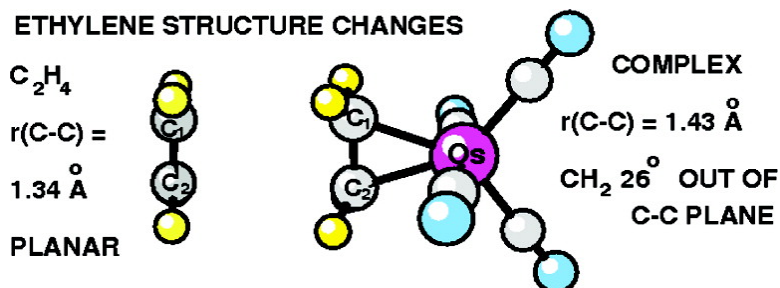


Structure of Tetracarbonylethyleneosmium: Ethylene Structure Changes upon Complex Formation

Chandana Karunatilaka, Brandon S. Tackett, John Washington, and Stephen G. Kukolich

J. Am. Chem. Soc., **2007**, 129 (34), 10522-10530 • DOI: 10.1021/ja0727969 • Publication Date (Web): 03 August 2007

Downloaded from <http://pubs.acs.org> on February 15, 2009



More About This Article

Additional resources and features associated with this article are available within the HTML version:

- Supporting Information
- Links to the 3 articles that cite this article, as of the time of this article download
- Access to high resolution figures
- Links to articles and content related to this article
- Copyright permission to reproduce figures and/or text from this article

[View the Full Text HTML](#)

Structure of Tetracarbonylethyleneosmium: Ethylene Structure Changes upon Complex Formation

Chandana Karunatilaka,[†] Brandon S. Tackett,[†] John Washington,[‡] and Stephen G. Kukolich^{*,†}

Contribution from the Departments of Chemistry, The University of Arizona, Tucson, Arizona 85721, and Concordia University College of Alberta, Edmonton, Alberta, Canada T5B 4E4

Received April 22, 2007; E-mail: kukolich@u.arizona.edu

Abstract: Rotational spectra of seven isotopomers of tetracarbonylethyleneosmium, $\text{Os}(\text{CO})_4(\eta^2\text{-C}_2\text{H}_4)$, were measured in the 4–12 GHz range using a Flygare–Balle-type pulsed-beam Fourier transform microwave spectrometer system. Olefin–transition metal complexes of this type occur extensively in recent organic syntheses and serve as important models for transition states in the metal-mediated transformations of alkenes. Three osmium (^{192}Os , ^{190}Os , and ^{188}Os) and three unique ^{13}C isotopomers (^{13}C in ethylene, axial, and equatorial positions) were observed in natural abundance. Additional spectra were measured for a perdeuterated sample, $\text{Os}(\text{CO})_4(\eta^2\text{-C}_2\text{D}_4)$. The measured rotational constants for the main osmium isotopomer (^{192}Os) are $A = 929.3256(6)$, $B = 755.1707(3)$, and $C = 752.7446(3)$ MHz, indicating a near-prolate asymmetric top molecule. The ~ 140 assigned b -type transitions were fit using a Watson S -reduced Hamiltonian including A , B , C , and five centrifugal distortion constants. A near-complete r_0 gas-phase structure has been determined from a least-squares structural fit using eight adjustable structural parameters to fit the 21 measured rotational constants. Changes in the structure of ethylene on coordination to $\text{Os}(\text{CO})_4$ are large and well-determined. For the complex, the experimental ethylene C–C bond length is 1.432(5) Å, which falls between the free ethylene value of 1.3391(13) Å and the ethane value of 1.534(2) Å. The angle between the plane of the CH_2 group and the extended ethylene C–C bond (\angle out-of-plane) is 26.0(3)°, indicating that this complex is better described as a metallacyclopropane than as a π -bonded olefin–metal complex. The Os–C–C–H dihedral angle is 106.7(2)°, indicating that the ethylene carbon atoms have near sp^3 character in the complex. Kraitchman analysis of the available rotational constants gave principal axis coordinates for the carbon and hydrogen atoms in excellent agreement with the least-squares fit results. The new results on this osmium complex are compared with earlier work on the similar complex, tetracarbonylethyleneiron ($\text{Fe}(\text{CO})_4(\eta^2\text{-C}_2\text{H}_4)$). The ethylene structural changes upon coordination to the metal are found to be larger for the ethylene–osmium complex than for the analogous ethylene–iron complex, consistent with the expected greater π donation for the osmium atom.

I. Introduction

The synthesis, structure, bonding, and reactivity of transition metal–alkene compounds have occupied a central place in organometallic chemistry.^{1–4} It is well recognized that the nature of the metal–alkene bond has a profound influence on the catalytic activity of the metal complexes and the reactivity of the coordinated alkene.^{5,6} The attachment of an alkene and polyenes to a transition metal atom results in significant

structural changes and enhances its reactivity toward nucleophilic attack;^{7–9} the latter feature has been extremely useful for organic synthesis.^{10,11} In addition, metal–alkene and metallacycloalkane compounds have been proposed as models for the chemisorption of organic species on the surface of heterogeneous catalysts¹² and can be useful for correlating IR spectra of the surface species with the free metallacycle complex.¹³ In the present work, we focus on the structure changes of ethylene when coordinated to a transition metal.

[†] The University of Arizona.

[‡] Concordia University College of Alberta.

- (1) Collman, J. P.; Hegedus, L. S.; Norton, J. R.; Finke, R. G. *Principles and Applications of Organotransitionmetal Chemistry*, 2nd ed.; University Science Books: Mill Valley, CA, 1987.
- (2) Crabtree, R. H. *The Organometallic Chemistry of Transition Metals*; Wiley: New York, 1986.
- (3) Yamamoto, A. *Organotransition Metal Chemistry*; Wiley: New York, 1986.
- (4) Geoffroy, G. L.; Wrighton, M. S. *Organometallic Photochemistry*; Academic Press: New York, 1979.
- (5) Parshall, G. W.; Iteel, S. D. *Homogeneous Catalysis*, 2nd ed.; Wiley-Interscience: New York, 1992.
- (6) van Leeuwen, P. W. N. M. *Homogeneous Catalysis—Understanding the Art*; Kluwer Academic Publishers: Dordrecht, 2004.

- (7) Bochmann, M. *Organometallics 2, Complexes with Transition Metal–Carbon π -Bonds*; Oxford Science Publications: Oxford, 1994; Chapter 2.
- (8) Kukolich, S. G. *J. Am. Chem. Soc.* **1995**, *117*, 5512–5514.
- (9) Pearson, A. J. *Metallo-Organic Chemistry*; John Wiley & Sons: New York, 1985; Chapter 9.
- (10) Collman, J. P.; Hegedus, L. S.; Norton, J. R.; Finke, R. G. *Principles and Applications of Organotransition Metal Chemistry*, 2nd ed.; University Science Books: Mill Valley, CA, 1987; Chapters 3 and 17.
- (11) Jones, G. B.; Heaton, S. B. *Tetrahedron: Asymmetry* **1993**, *4*, 261.
- (12) Sheppard, N. *Annu. Rev. Phys. Chem.* **1988**, *39*, 589.
- (13) Anson, C. E.; Sheppard, N.; Powell, D. B.; Bender, B. R.; Norton, J. R. *J. Chem. Soc., Faraday Trans.* **1994**, *90*, 1449.

The model to describe alkene bonding to a transition metal, proposed by Dewar¹⁴ over 50 years ago, has been proven to provide a quite useful correlation of structural changes and orbital interactions. The model was successfully applied by Chatt and Duncanson¹⁵ for a systematic description of metal–olefin complexes and is now termed the DCD model. Dewar¹⁶ suggested the existence of two extremes of the metal–olefin bond character, ranging from a “simple π -complex” to a metallacyclopropane, similar to the classical, strained three-membered ring. Metal–olefin bonds generally fall somewhere between the two extremes.¹⁶ The DCD model provides a useful qualitative description of the bonding, but density functional theory (DFT) calculations are now readily available which provide remarkably accurate quantitative structural and bonding details. Frenking has used an energy partitioning analysis to validate the DCD model in terms of quantitative molecular orbital calculations.¹⁷ Scherer et al.¹⁸ reported a charge density analysis, with graphic illustrations of charge redistribution for ethylene–nickel bonding, in support of the DCD model.

The structure and bonding of tetracarbonylethyleneosmium, $\text{Os}(\text{CO})_4(\eta^2\text{-C}_2\text{H}_4)$, have been investigated previously, predominantly by Norton and co-workers.^{19–21} In 1992,¹⁹ they published results from ¹H NMR spectra, single-crystal X-ray diffraction measurements, and Hartree–Fock *ab initio* calculations. A comparison of the spin–spin coupling constants of the complex versus those of free ethylene indicated a significant rehybridization of the ligand (specifically, a decrease in the H–C–H angle and an increase in the C–C bond length) upon coordination to the metal. The X-ray results confirmed the expected “trigonal bipyramidal” geometry of the complex, giving bond lengths and angles in general agreement with their *ab initio* results, except for the rather long, and relatively uncertain, ethylene C–C bond length of 1.488(24) Å versus a Hartree–Fock value of 1.44 Å. Accurate H-atom coordinates could not be obtained from the X-ray data. In 1994,¹³ Anson et al. performed a comprehensive vibrational assignment of the hydrocarbon features in the infrared and Raman spectra of the complex and its (¹³C₂H₄) and (C₂D₄) isotopomers, which further indicated its metallacyclopropane nature. A liquid-crystal ¹H NMR study was carried out by Bender et al.¹⁹ to determine the bond lengths and bond angles adjacent to the ethylene carbons in a nematic-phase solution. After correcting their experimental structural parameters for harmonic vibrational contributions, they obtained $r_{\text{CH}} = 1.083(2)$ Å, $\angle_{\text{HCH}} = 113.48(5)^\circ$, and the angle between the plane of the CH₂ group and the extended C–C bond, $\angle_{\text{out-of-plane}} = 31.27(2)^\circ$.

Extensive DFT calculations have been performed for the ethylene carbonyl complexes of the group 8 transition metals ($\text{M}(\text{CO})_4(\eta^2\text{-C}_2\text{H}_4)$; M = Fe, Ru, Os). Li and co-workers²² have illustrated the effect of relativity on the metal–olefin bond

strength and the structural deformation of the ethylene ligand for d⁸ complexes with larger nuclear charge. Nechaev et al.²³ have used an energy decomposition analysis (EDA) method to estimate the ratio of electrostatic and covalent bonding present in the group 8 ethylene carbonyl complexes. These calculations allowed the authors to further partition the metal–ethylene bond into the individual contributions from the irreducible representations of the system point group (C_{2v}). For $\text{Os}(\text{CO})_4(\eta^2\text{-C}_2\text{H}_4)$, they obtained a $\sigma(a_1)$ contribution of 42.4% and a $\pi_{\parallel}(b_2)$ contribution of 53.3% (minor $\pi_{\perp}(b_1)$ and $\delta(a_2)$ contributions comprised the 4.3% balance). The analysis indicated significant metal d _{π} -to-ligand π^* back-bonding and therefore metallacyclopropane character.

The formation of transition metal complexes with alkenes and many other organic molecules causes large and significant changes in the structure and reactivity of the organic ligand. In the present work, we have used Fourier transform microwave (FTMW) spectroscopy measurements of seven unique $\text{Os}(\text{CO})_4(\eta^2\text{-C}_2\text{H}_4)$ isotopomers to obtain the first nearly complete, gas-phase structure of this complex, including accurate and precise ethylene carbon and hydrogen atom coordinates. From the available data, we have determined two consistent sets of structural parameters, using the Kraitchman relations and a least-squares structure-fit analysis. The present and earlier^{22,23} DFT calculations are in excellent agreement with these experimental results. The new results on this osmium complex are compared with the earlier FT microwave spectroscopy work on the iron-containing congener, tetracarbonylethyleneiron²⁴ ($\text{Fe}(\text{CO})_4(\eta^2\text{-C}_2\text{H}_4)$), and the dihydride complex, tetracarbonyldihydroosmium²⁵ ($\text{H}_2\text{Os}(\text{CO})_4$), and with previous studies of the title complex. These results clearly illustrate the extent to which coordination to a metal center can modify the structure of the coordinated olefin.

II. Experiment

(a) Sample Preparation. The first synthesis and characterization of $\text{Os}(\text{CO})_4(\eta^2\text{-C}_2\text{H}_4)$ (**1**) was reported by Norton et al.²⁶ in 1982. A more direct and efficient synthesis is via photolysis of either $\text{Os}_3(\text{CO})_{12}$ ^{27,28} or $\text{Os}(\text{CO})_5$.²⁹ When $\text{Os}(\text{CO})_5$ is available, the synthesis given by Kiel and Takats²⁹ is preferred, and this procedure was used in the present work to prepare **1** and $\text{Os}(\text{CO})_4(\eta^2\text{-C}_2\text{D}_4)$ (**1-d₄**).

All procedures were carried out using standard Schlenk techniques under a nitrogen atmosphere. Pentane (HPLC grade) was purchased from Caledon Laboratories and was distilled from CaH₂ immediately prior to use. Ethylene was purchased from Linde, and ethylene-*d*₄ (99% atom D) was purchased from Isotec. Both were used as received. The $\text{Os}(\text{CO})_5$ used in the synthesis was prepared by a published procedure.^{30,31}

The samples were characterized using infrared spectra obtained on a Bomem MB-100 Fourier transform spectrometer over the range

(14) Dewar, M. J. S. *Bull. Soc. Chim. Fr.* **1951**, 18, C71.

(15) Chatt, J.; Duncanson, L. A. *J. Chem. Soc.* **1953**, 2939.

(16) Dewar, M. J. S.; Ford, G. P. *J. Am. Chem. Soc.* **1979**, 101, 783.

(17) (a) Frenking, G. *J. Organomet. Chem.* **2001**, 635, 9. (b) Frenking, G. In *Modern Coordination Chemistry: The Legacy of Joseph Chatt*; Leigh, G. J., Winterton, N., Eds.; The Royal Society: London, 2002; p 111.

(18) Scherer, W.; Eickerling, G.; Shorokhov, D.; Gullo, E.; McGrady, G. S.; Sirsch, P. *New J. Chem.* **2006**, 30, 309–312.

(19) Bender, B. R.; Norton, J. R.; Miller, M. M.; Anderson, O. P.; Rappe, A. K. *Organometallics* **1992**, 11, 3427.

(20) Anson, C. E.; Sheppard, N.; Powell, D. B.; Bender, B. R.; Norton, J. R. *J. Chem. Soc., Faraday Trans.* **1994**, 90, 1449.

(21) Bender, B. R.; Hembre, R. T.; Norton, J. R.; Burnell, E. E. *Inorg. Chem.* **1998**, 37, 1720.

(22) Li, J.; Schreckenbach, G.; Ziegler, T. *Inorg. Chem.* **1995**, 34, 3245.

(23) Nechaev, M. S.; Rayón, V. M.; Frenking, G. *J. Phys. Chem. A* **2004**, 108, 3134.

(24) Drouin, B. J.; Kukolich, S. G. *J. Am. Chem. Soc.* **1999**, 121, 4023.

(25) Kukolich, S. G.; Sickafoose, S. M.; Breckenridge, S. M. *J. Am. Chem. Soc.* **1996**, 118, 205.

(26) Carter, W. J.; Kelland, J. W.; Okrasinski, S. J.; Warner, K. E.; Norton, J. R. *Inorg. Chem.* **1982**, 21, 3955–3960.

(27) Bender, B. R.; Norton, J. R.; Miller, M. M.; Anderson, O. P.; Rappe, A. K. *Organometallics* **1992**, 11, 3427.

(28) Burke, M. R.; Takats, J.; Grevels, F.-W.; Reuvers, J. G. A. *J. Am. Chem. Soc.* **1983**, 105, 4092.

(29) Kiel, G. Y.; Takats, J.; Grevels, F. W. *J. Am. Chem. Soc.* **1987**, 109, 2227.

(30) Washington, J.; McDonald, R.; Takats, J.; Menashe, N.; Reshef, D.; Shvo, Y. *Organometallics* **1995**, 14, 3996.

(31) Rushman, P.; Van Buuren, G. N.; Shiralian, M.; Pomeroy, R. K. *Organometallics* **1983**, 2, 693–694.

2200–1600 cm^{-1} . All FT-IR spectra were obtained as solution samples held between KBr (0.1 mm) plates.

The photochemical syntheses were carried out using the immersion well described in ref 30, and illustrated in the Supporting Information. The immersion well has an approximate solution volume of 100 mL. The immersion well consists of an outside cooling jacket, two ports for the cooling solution, a gas inlet, two ports for solution sampling, and a cooling insert into which the lamp is placed. The irradiation source was a Philips HPK 125 W mercury vapor lamp, and the wavelength of the radiation was controlled using a cutoff filter ($\lambda > 370$ nm) fashioned from Glaswerk Wertheim glass. A Julabo F83 circulating bath was used to circulate ethanol through the photochemical apparatus, maintaining the reaction solution at the desired temperature while keeping the lamp cool. Reaction progress was measured by periodically removing small amounts (*ca.* 0.2 mL) of reaction solution with a 1-mL syringe and recording the FT-IR spectrum.

(b) Preparation of $\text{Os}(\text{CO})_4(\eta^2\text{-C}_2\text{H}_4)$ (1**).** The preparation used herein is a minor modification of the previously published synthesis of **1** from $\text{Os}(\text{CO})_5$, using pentane, rather than butane, as the reaction solvent. The photochemical immersion well was charged with a pentane solution containing $\text{Os}(\text{CO})_5$ (234 mg, 0.708 mmol) and the solution volume adjusted to 90 mL using freshly distilled pentane. The temperature of the immersion well was maintained at -40 °C, and ethylene was bubbled through the solution via the gas inlet for 10 min (approximately 1 bubble/s) prior to photolysis. The cooled solution was then photolyzed for 55 min while maintaining constant ethylene bubbling. The reaction was deemed complete when no $\nu(\text{CO})$ peaks due to $\text{Os}(\text{CO})_5$ were present and only $\nu(\text{CO})$ bands due to **1** were observed in the FT-IR spectrum. The resulting pentane solution containing **1** was transferred by cannula to a flask precooled to -78 °C. Care was taken to avoid subjecting solutions of **1** to ambient light, and all subsequent operations were carried out under darkened conditions. The solvent and excess ethylene were removed *in vacuo* at -60 °C to yield a yellow-brown residue. The contents of the flask were then distilled at room temperature under static vacuum (0.05 Torr) to a Schlenk tube cooled with liquid nitrogen, affording **1** in 80% yield (188 mg, 0.569 mmol).

(c) Preparation of $\text{Os}(\text{CO})_4(\eta^2\text{-C}_2\text{D}_4)$ (1-d₄**).** The characterization of $\text{Os}(\text{CO})_4(\eta^2\text{-C}_2\text{D}_4)$ (**1-d₄**) has been reported previously.³² Compound **1-d₄** was synthesized via the method described for **1**. The immersion well was charged with a pentane solution containing $\text{Os}(\text{CO})_5$ (204 mg, 0.618 mmol) and the solution volume adjusted to 90 mL using freshly distilled pentane. The temperature of the immersion well was maintained at -40 °C, and ethylene-*d*₄ was bubbled through the solution via the gas inlet for 2 min (approximately 1 bubble/s) prior to photolysis. The cooled solution was then photolyzed for 2 h while maintaining a slow nitrogen purge (approximately one bubble every 3 s). At approximately 15-min intervals during the photolysis, the nitrogen purge was stopped and ethylene-*d*₄ was bubbled through the reaction solution for 20 s, after which time the slow nitrogen purge was resumed. The reaction was deemed complete when no $\nu(\text{CO})$ peaks due to $\text{Os}(\text{CO})_5$ were present and only $\nu(\text{CO})$ IR bands due to **1-d₄** were observed. The $\nu(\text{CO})$ bands of **1-d₄** were identical to those for **1**, consistent with results reported by Norton and co-workers.³² After complete photolysis, the resulting reaction solution contained suspended yellow-brown particles, ascribed to the photochemical decomposition of $\text{Os}(\text{CO})_5$. The longer photolysis time and evidence of $\text{Os}(\text{CO})_5$ decomposition are likely the result of the lower concentration of ethylene-*d*₄, as compared to ethylene, during the photochemical reaction to produce **1-d₄**. The isolation of **1-d₄** was carried out as described for **1**, with **1-d₄** isolated in 49% yield (101 mg, 0.302 mmol).

(d) Rotational Spectra. Rotational transitions of $\text{Os}(\text{CO})_4(\eta^2\text{-C}_2\text{H}_4)$ were measured in the 4–12 GHz range using a Flygare–Balle-type

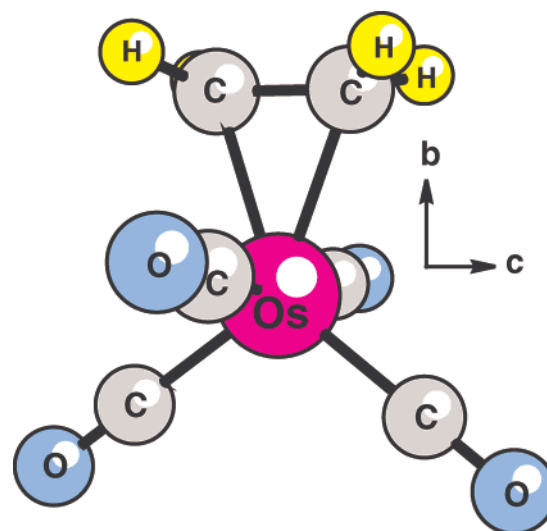


Figure 1. Molecular structure and principal axis system for tetracarbonyl-ethyleneosmium. As shown, axial carbons are staggered with the ethylene carbons and are at an angle of $4.1(5)^\circ$ relative to the *a* axis.

pulsed-beam Fourier transform microwave spectrometer system, which is described elsewhere.³³ Caution was used when handling the samples as the complex is sensitive to light, heat, moisture, and air. Both the normal and perdeuterated samples were maintained at -15 to -20 °C (using an ethanol/water dry ice slush bath) during the experiment to limit their vapor pressure. Research-grade neon was employed as carrier gas at a backing pressure of 0.7–0.8 atm. Gas pulses were injected transversely into the microwave cavity (background pressure = 10^{-6} Torr) at a rate of 1–2 Hz using a pulsed valve (General Valve, Series 9, 2 mm orifice). The superheterodyne microwave detection system used previously was replaced by a new homodyne detection system which has been explained in detail in a recent paper.³⁴ The most intense transitions of the main and the multiply substituted $\text{Os}(\text{CO})_4(\eta^2\text{-C}_2\text{D}_4)$ isotopomers could be detected within a single gas pulse. The line widths obtained (fwhm) were ~ 30 kHz for well-resolved lines and yielded measurement uncertainties 1–6 kHz.

III. DFT Calculations

Extensive density functional theory calculations were performed using the Gaussian 03 program suite³⁵ to optimize the equilibrium geometry and produce preliminary rotational constants prior to searching for molecular rotational transitions. Results from our best calculations are reported in Table 4 (below) and were obtained using Becke's three-parameter hybrid exchange potential (B3)³⁶ with the Perdew–Wang (PW91)³⁷ gradient-corrected correlation functional. Dunning's correlation-consistent triple- ζ basis sets augmented by diffuse functions (aug-cc-pVTZ)³⁸ were employed for carbon, hydrogen, and oxygen, while the Hay–Wadt VDZ (n+1) ECP³⁹ was chosen for osmium. All geometry optimizations were followed by a frequency analysis to ensure that the stationary points found were true minima on the potential energy surface. Figure 1 illustrates the DFT-calculated geometry of the complex in the principal axis system. The ethylene group is bound on one of the equatorial sites of a nearly trigonal bipyramidal structure, and the C–C bond lies in the equatorial plane. The molecule possesses C_{2v} symmetry, with the *b*-axis coinciding with the two-fold rotation axis bisecting the ethylene C–C bond. The “axial” carbonyl ligands, which

(33) Bumgarner, R. E.; Kukolich, S. G. *J. Chem. Phys.* **1987**, *86*, 1083.

(34) Tackett, B. S.; Karunatilaka, C.; Daly, A.; Kukolich, S. G. *Organometallics* **2007**, *26*, 2070–2076.

(35) Frisch, M. J.; et al. *Gaussian 03*, Revision C.02; Gaussian Inc.: Willingford, CT, 2004.

(36) Beck, A. D. *J. Chem. Phys.* **1993**, *98*, 5648.

(37) Perdew, J. P.; Burke, K.; Wang, Y. *Phys. Rev. B* **1996**, *54*, 16533.

(38) Dunning, T. H., Jr. *J. Chem. Phys.* **1989**, *90*, 1007.

(39) Hay, P. J.; Wadt, W. R. *J. Chem. Phys.* **1985**, *82*, 299.

(32) Bender, B. R.; Ramage, D. L.; Norton, J. R.; Wisner, D. C.; Rappé, A. K. *J. Am. Chem. Soc.* **1997**, *119*, 5628.

are staggered with respect to the ethylene carbons, lie in the *ab* plane and are angled slightly ($\sim 4^\circ$) toward the ethylene ligand. The “equatorial” carbonyl ligands are eclipsed with the ethylene carbons and lie in the *bc* mirror plane with a C–Os–C angle of $\sim 105^\circ$. The normal isotopomer has a calculated dipole moment of 1.32 D, oriented completely along the *b* principal axis. The DFT structural parameters are reported in Table 8 (below) for comparison with experimental values.

The capability of Gaussian 03 to do numerical differentiation along the normal vibrational modes to determine anharmonic vibrational parameters for DFT methods was used to calculate quartic centrifugal distortion constants. The rotational parameters obtained from this calculation are given in Table 4 (below), along with the experimental values for comparison.

IV. Results and Data Analysis

Using the preliminary rotational constants obtained from the DFT calculations, Pickett’s SPCAT program⁴⁰ was used to predict the *b*-type transition frequencies with selection rules $\Delta J = 0, \pm 1, \Delta K_a = \pm 1, \Delta K_c = \pm 1, \pm 3$. As illustrated in Table 4, the rotational constants for the normal isotopomer obtained from the DFT calculations agree remarkably well with the experimentally obtained values. This drastically simplified the initial search for lines; in fact, the first transition measured ($J'_{K'_a K'_c} \leftarrow J''_{K''_a K''_c} = 6_{16} \leftarrow 5_{05}$), at 9197.8522 MHz, deviated only 1.5 MHz from the frequency predicted from the calculation. There are four osmium isotopes with appreciable natural abundances (^{188}Os 13.2%, ^{189}Os 16.2%, ^{190}Os 26.3%, and ^{192}Os 40.8%), with only ^{189}Os having a nonzero nuclear spin ($I = 3/2$). Figure 2a illustrates the $4_{14} \leftarrow 3_{03}$ transitions at ~ 6195 MHz observed using the normal $\text{Os}(\text{CO})_4(\eta^2\text{-C}_2\text{H}_4)$ sample. Similar three-line patterns were observed for most of the $\Delta K_a = +1$ transitions. Comparing the observed isotope splittings with those predicted by DFT calculations for the various osmium-substituted isotopomers indicated that these persistent triads are due to ^{188}Os , ^{190}Os , and ^{192}Os species. The energy level splitting due to the ^{189}Os nuclear quadrupole coupling presumably makes the spectrum of this isotopomer too weak to be observed. Figure 2b shows the $4_{04} \leftarrow 3_{13}$ transitions in which lines from the different osmium isotopomers are completely overlapped. This was the case for many of the $\Delta K_a = -1$ transitions, and in such overlapped cases the center frequency was assigned to the most abundant ^{192}Os species. For the C_2D_4 -ethylene isotopomer, the center of mass for the complex is shifted along the *b*-axis to a point even closer to the osmium atom. This decreased the observed isotope splitting, leading to broader, unresolved lines in most cases. The quadrupole coupling resulting from the four deuterium nuclei ($I = 1$) must also contribute to the observed line width, as the splitting was not resolvable. Thus, we decided to choose the center frequency for many of the broadened, poorly resolved lines and to assign only the $^{192}\text{Os}-\text{D}_4$ isotopomer transitions. Nearly 140 “*b*-type” dipole transitions were measured for the various osmium, perdeuterated, and ^{13}C (2.1% natural abundance) isotopomers in the 4–12 GHz range. No ^{18}O transitions were observed in the present study.

The measured transitions were fitted using a rigid-rotor Hamiltonian with centrifugal distortion constants with Pickett’s SPFIT fitting program,⁴⁰ and the results are listed in Tables 1–3, along with the fit residuals from the fit. The molecule is a very nearly prolate asymmetric top, and the 42 observed transitions

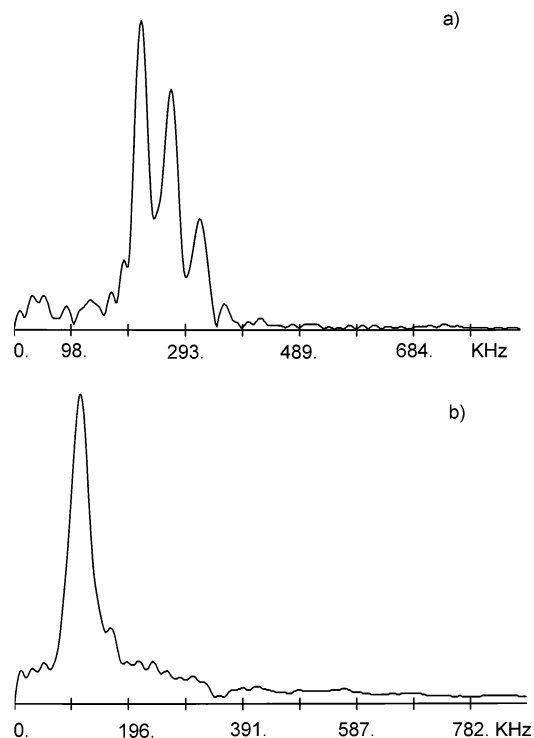


Figure 2. (a) Observed spectrum of $\text{Os}(\text{CO})_4(\eta^2\text{-C}_2\text{H}_4)$ corresponding to the $J'_{K'_a K'_c} \leftarrow J''_{K''_a K''_c} = 4_{14} \leftarrow 3_{03}$ transition at ~ 6195 MHz, showing lines from three osmium isotopes (^{188}Os , ^{190}Os , and ^{192}Os). (b) Spectrum observed for the $J'_{K'_a K'_c} \leftarrow J''_{K''_a K''_c} = 4_{04} \leftarrow 3_{13}$ transition at ~ 5863 MHz. The somewhat broader spectrum (b) is due to overlapped lines arising from the different osmium isotopes. The frequency scales are in kilohertz, relative to the (arbitrary) stimulating frequency.

for the most abundant ^{192}Os isotopomer were fitted using a Watson *S*-reduced Hamiltonian in the I^r representation, including rotational parameters $A, B, C, D_J, D_{JK}, D_K, d_1,$ and d_2 . For the $^{190}\text{Os}(\text{CO})_4(\eta^2\text{-C}_2\text{H}_4)$, $^{188}\text{Os}(\text{CO})_4(\eta^2\text{-C}_2\text{H}_4)$, and $^{192}\text{Os}(\text{CO})_4(\eta^2\text{-C}_2\text{H}_4)$ species, $A, B, C, D_J,$ and D_K were fitted while $D_{JK}, d_1,$ and d_2 were held fixed at the values obtained for the normal isotopomer. Due to the limited data sets (see Table 3) obtained for the ^{13}C -substituted isotopomers, all of the distortion constants were held fixed at the values obtained for the normal (^{192}Os) isotopomer. Table 4 summarizes the rotational parameters obtained from the analyses of all the isotopomers. We note that the centrifugal distortion constants are quite small, indicating that the molecule has a fairly rigid structure. The rotational parameters obtained from DFT calculations, including the distortion constants, are in excellent agreement with the experimental results (see Table 4).

V. Molecular Structure

(a) Least-Squares Structural Fit. In the present study, a total of 21 rotational constants have been determined for various isotopomers of tetracarbonylethyleneosmium, and these constants were used to obtain r_0 structural parameters for this molecule. The least-squares structural fits were done by adjusting the structural parameters to obtain the best fit to the 21 rotational constants. Because we have not measured spectra corresponding to isotopic substitution at every unique atom in the complex, we had to use a few constraints on the structure for the least-squares structure-fit analysis. The predicted $\angle\text{Os}-\text{C}-\text{O}$ angles from DFT calculations for the axial and equatorial carbonyl ligands are 178.1° and 179.7° , respectively;

(40) Pickett, H. M. *J. Mol. Spectrosc.* **1991**, *148*, 371–377.

Table 1. Measured Transition Frequencies for the Most Abundant ($C_2H_4^{192}Os(CO)_4$, 41% Natural Abundance) and Perdeuterated ($C_2D_4^{192}Os(CO)_4$), Isotopomers with the Deviations from Calculated Values (in MHz)

quantum nos. $J_{K_a/K_c} J_{K_b/K_c}$	$C_2H_4Os(CO)_4$		$C_2D_4Os(CO)_4$	
	measured	dev	measured	dev
3 ₀₃ 2 ₁₂			4279.3493	0.0016
3 ₁₃ 2 ₀₂	4691.8402	0.0001	4494.0882	-0.0079
3 ₂₂ 2 ₁₁	5046.1990	-0.0040	4817.4604	0.0050
3 ₂₁ 2 ₁₂	5053.5943	-0.0098	4887.7100	-0.0051
3 ₃₁ 2 ₂₀	5400.5692	-0.0030	5140.8174	-0.0003
3 ₃₀ 2 ₂₁			5142.9918	-0.0014
4 ₁₄ 3 ₂₁	5493.2144	-0.0162		
4 ₁₃ 3 ₂₂	5517.6240	0.0116		
4 ₀₄ 3 ₁₃	5863.2021	-0.0001	5760.1590	-0.0051
4 ₁₄ 3 ₀₃	6194.9470	0.0002	5927.0890	-0.0003
4 ₂₃ 3 ₁₂	6550.4697	0.0039	6255.9156	0.0012
4 ₂₂ 3 ₁₃	6565.3967	0.0039	6405.4907	-0.0027
4 ₃₂ 3 ₂₁	6908.4219	0.0012	6605.2869	0.0009
4 ₃₁ 3 ₂₂	6908.5476	0.0015	6616.2813	-0.0018
4 ₄₁ 3 ₃₀	7259.2318	-0.0019	6904.7747	-0.0033
4 ₄₀ 3 ₃₁			6904.9129	-0.0030
5 ₁₅ 4 ₂₂	6994.7393	0.0021		
5 ₁₄ 4 ₂₃	7031.4965	-0.0001		
5 ₀₅ 4 ₁₄	7375.5146	0.0046	7237.0612	0.0017
5 ₁₅ 4 ₀₄	7696.9273	-0.0006	7357.3389	0.0039
5 ₂₄ 4 ₁₃	8053.5108	0.0004		
5 ₂₃ 4 ₁₄	8078.6410	0.0032	7949.2656	0.0042
5 ₃₃ 4 ₂₂	8416.1696	0.0017		
5 ₃₂ 4 ₂₃	8416.5456	0.0003		
5 ₄₂ 4 ₃₁	8767.1250	0.0003	8373.5876	0.0040
5 ₄₁ 4 ₃₂			8374.5586	0.0008
6 ₂₅ 5 ₃₂	8170.2777	-0.0147		
6 ₂₄ 5 ₃₃	8172.0400	0.0049		
6 ₁₆ 5 ₂₃	8494.7217	-0.0027		
6 ₁₅ 5 ₂₄	8546.5252	-0.0082		
6 ₀₆ 5 ₁₅	8888.7135	0.0027	8707.7804	0.0032
6 ₁₆ 5 ₀₅	9197.8522	0.0000	8788.5977	0.0008
6 ₂₅ 5 ₁₄	9555.3418	0.0007	9104.4326	0.0006
6 ₂₄ 5 ₁₅	9593.4625	-0.0033		
6 ₃₄ 5 ₂₃	9923.7433	-0.0011		
6 ₄₂ 5 ₃₃			9844.6908	0.0031
6 ₄₃ 5 ₃₂	10275.0000	-0.0002	9840.7721	-0.0009
7 ₂₆ 6 ₃₃	9677.8785	0.0075		
7 ₂₅ 6 ₃₄	9680.9990	-0.0092		
7 ₁₇ 6 ₂₄	9993.0541	0.0015		
7 ₀₇ 6 ₁₆	10402.6847	-0.0019	10172.0773	-0.0024
7 ₁₇ 6 ₀₆	10697.8051	-0.0025	10223.2867	0.0026
7 ₂₆ 6 ₁₅	11055.9669	0.0018		
7 ₂₅ 6 ₁₆	11110.0227	-0.0055		
7 ₄₄ 6 ₃₃	11782.8555	0.0031		
8 ₀₈ 7 ₁₇	11917.3017	-0.0015	11631.0352	-0.0045
8 ₁₈ 7 ₀₇	12196.9002	0.0001		

we have constrained them both to 180° . Furthermore, the DFT-calculated equatorial C–O bond distance is 1.1437 Å, while the corresponding axial bond distance is 1.1385 Å. The respective carbonyl bond distances were fixed to these DFT-calculated values in the least-squares fit, since no data for ^{18}O isotopomers were obtained in the present study. We also tried including the C_{et} –H bond distance as an adjustable parameter, but this resulted in a large (and unreasonable) value for the ethylene C–C bond distance (1.49 Å) and more serious correlations among the ethylene group structural parameters. Consequently, this C_{et} –H bond distance was held fixed to the DFT value of 1.083 Å during the fit. With the structure constrained to C_{2v} symmetry, this scheme allowed variation of eight independent structural parameters in a fit to the 21 measured rotational constants, and these parameters were found to be the best determinable set. The parameters are (1) the distance from osmium to the axial carbon, $r(Os-C_{ax})$; (2) the

Table 2. Measured Rotational Transition Frequencies and Fit Residuals for ^{190}Os (26%) and ^{188}Os (13%) Isotopes of Tetracarbonyl ethyleneosmium (All Frequencies in MHz)

quantum nos. $J_{K_a/K_c} J_{K_b/K_c}$	$C_2H_4^{190}Os(CO)_4$		$C_2H_4^{188}Os(CO)_4$	
	measured	dev	measured	dev
3 ₁₃ 2 ₀₂	4691.8750	0.0016	4691.9092	-0.0006
3 ₂₂ 2 ₁₁	5046.2300	-0.0081	5046.2700	0.0072
3 ₂₁ 2 ₁₂	5053.6120	-0.0080	5053.6400	0.0022
4 ₁₄ 3 ₀₃	6194.9990	0.0029	6195.0483	-0.0003
4 ₂₃ 3 ₁₂	6550.5164	0.0021	6550.5656	0.0007
5 ₁₅ 4 ₂₂	6994.7832	-0.0044	6994.8380	0.0011
5 ₁₄ 4 ₂₃	7031.4500	0.0014		
4 ₄₁ 3 ₃₀	7259.2778	-0.0003	7259.3326	-0.0005
5 ₁₅ 4 ₀₄	7697.0000	0.0032	7697.0686	0.0005
5 ₂₄ 4 ₁₃	8053.5765	0.0002	8053.6484	0.0039
6 ₂₅ 5 ₃₂	8170.2940	0.0031		
5 ₃₃ 4 ₂₂	8416.2118	-0.0005	8416.2646	0.0051
5 ₃₂ 4 ₂₃	8416.5887	0.0019	8416.6338	0.0021
6 ₁₆ 5 ₂₃	8494.8004	-0.0030	8494.8906	0.0118
6 ₁₅ 5 ₂₄	8546.4710	0.0024		
6 ₀₆ 5 ₁₅	8888.6840	-0.0018		
6 ₁₆ 5 ₀₅	9197.9457	0.0012	9198.0461	0.0098
6 ₂₅ 5 ₁₄	9555.4316	0.0025	9555.5227	0.0066
6 ₃₄ 5 ₂₃	9923.7991	0.0032	9923.8400	-0.0064
7 ₁₇ 6 ₂₄	9993.1680	-0.0004	9993.2832	0.0082
7 ₁₆ 6 ₂₅	10062.6140	-0.0024		
7 ₁₇ 6 ₀₆	10697.9290	0.0022	10698.0503	0.0098
7 ₂₆ 6 ₁₅	11056.0781	-0.0024	11056.1943	0.0051
8 ₁₈ 7 ₀₇	12197.0479	-0.0018		

distance from osmium to the equatorial carbon, $r(Os-C_{eq})$; (3) the distance from osmium to the ethylene carbon, $r(Os-C_{et})$; (4) the $C_{ax}-Os-C_{ax}$ angle; (5) the $C_{eq}-Os-C_{eq}$ angle; (6) the $C_{et}-Os-C_{et}$ angle; (7) the $H-C_{et}-H$ angle; and (8) the angle between the plane of the CH_2 group and the extended C–C bond ($\angle_{out-of-plane}$). The overall standard deviation for the least-squares structural fit was 15 kHz, which is an excellent result considering that the standard errors of the rotational analyses range from 3 to 6 kHz and portions of the structure were fixed to DFT values. The measured and calculated rotational constants (A , B , C) for various isotopomers of $Os(CO)_4(\eta^2-C_2H_4)$ are shown in Table 5, along with the fit residuals. The Cartesian coordinates (in Å) obtained in the principal axis system and all the structural parameters derived from the structural fit are presented in Tables 6 and 7, respectively. The estimated uncertainties are ± 0.010 – 0.020 Å for these coordinates, as most were not fitted directly. There were some fairly highly correlated parameters in the fit. The $r(Os-C_{ax})$ and $C_{ax}-Os-C_{ax}$ angle each have a correlation coefficient of 0.9996, with a similar value for the $r(Os-C_{eq})$ and $C_{eq}-Os-C_{eq}$ angle. However, the correlated structure-fit parameters obtained were confirmed by the Kraitchman analysis (*vide infra*), which is not hampered by such correlation problems. Table 7 also summarizes the structural parameters obtained from X-ray diffraction¹⁹ and our DFT calculations along with the FTMW values obtained for the $Fe(CO)_4(\eta^2-C_2H_4)$ ²⁴ congener and a similar complex, $H_2Os(CO)_4$.

(b) Kraitchman Analysis. A complete substitution (r_s) structure could not be obtained in the present study since we have not measured all the possible unique isotopomers for this complex (no ^{18}O isotopomers were measured in this work). Nevertheless, the more important hydrogen, carbon, and osmium atom coordinates were derived from a Kraitchman analysis,⁴¹

(41) Gordy, W.; Cook, R. L. *Microwave Molecular Spectra*, 3rd ed.; Wiley: New York, 1984; pp 661–664.

Table 3. Measured Transition Frequencies (in Natural Abundance, 2.1% in All Cases) and Deviations from Calculated Values for Various Unique ^{13}C -Substituted Isotopomers (in MHz)

quantum nos. $J_{K_a/K_c} J_{K_b/K_c}$	$^{13}\text{C}_1(\equiv\text{C}_3)$ axial		$^{13}\text{C}_2(\equiv\text{C}_4)$ equatorial		$^{13}\text{C}_5(\equiv\text{C}_6)$ ethylene	
	measured	dev	measured	dev	measured	dev
4 ₀₄ 3 ₁₃	5824.8839	-0.0130	5855.3945	0.0028	5858.8628	-0.0019
4 ₄₁ 3 ₃₀	7254.6050	0.0052				
5 ₀₅ 4 ₁₄			7366.1260	-0.0028	7371.8996	-0.0026
5 ₂₄ 4 ₁₃	8023.5117	0.0039	8012.0859	-0.0014	7981.1110	0.0069
5 ₂₃ 4 ₁₄			8055.8965	-0.0025	8067.7439	-0.0015
5 ₃₃ 4 ₂₂	8394.5918	-0.0084	8374.5058	-0.0071	8356.8545	-0.0011
5 ₃₂ 4 ₂₃	8394.9624	-0.0101	8375.6510	0.0097	8360.9759	0.0038
5 ₄₂ 4 ₃₁	8753.9660	-0.0056				
5 ₄₁ 4 ₃₂					8698.3507	0.0036
6 ₀₆ 5 ₁₅	8833.3720	-0.0013	8878.0036	0.0015	8885.6544	0.0043
6 ₁₆ 5 ₀₅	9150.8906	0.0057			9107.0651	-0.0044

Table 4. Rotational and Distortion Constants Obtained from the Least-squares Fits for All Measured Isotopomers. DFT Calculated Parameter Values Are Also Presented for Comparison Purposes. The Listed Errors Are 2σ .

parameter	$\text{C}_2\text{H}_4\text{Os}(\text{CO})_4$ (^{192}Os)	DFT ^a (^{192}Os)	$\text{C}_2\text{H}_4\text{Os}(\text{CO})_4$ (^{190}Os)	$\text{C}_2\text{H}_4\text{Os}(\text{CO})_4$ (^{188}Os)	$\text{C}_2\text{D}_4\text{Os}(\text{CO})_4$ (^{192}Os)	^{13}C axial (^{192}Os)	^{13}C equatorial (^{192}Os)	^{13}C ethylene (^{192}Os)
A (MHz)	929.3256(6)	930.85	929.3328(5)	929.3407(7)	881.4489(1)	929.2751(3)	923.1201(10)	920.6996(5)
B (MHz)	755.1707(3)	754.62	755.1689(2)	755.1666(7)	744.4294(1)	750.9077(2)	753.9757(4)	754.9994(3)
C (MHz)	752.7446(3)	752.56	752.7494(2)	752.7545(3)	724.3714(2)	748.4802(2)	749.8525(8)	747.2494(3)
D_J (kHz)	0.037(3)	0.05	0.033(3)	0.033(3)	0.035(1)	0.037(3) ^b	0.037(3) ^b	0.037(3) ^b
D_{JK} (kHz)	0.227(17)	0.21	0.227 ^b	0.227 ^b	0.227 ^b	0.227 ^b	0.227 ^b	0.227 ^b
D_K (kHz)	-0.29(3)	-0.24	-0.24(3)	-0.23(4)	-0.21(1)	-0.29 ^b	-0.29 ^b	-0.29 ^b
d_1 (kHz)	-0.002(2)	-0.002	-0.002 ^b	-0.002 ^b	-0.002 ^b	-0.002 ^b	-0.002 ^b	-0.002 ^b
d_2 (kHz)	0.0073(8)	-0.0066	0.0073 ^b	0.0073 ^b	0.0073 ^b	0.0073 ^b	0.0073 ^b	0.0073 ^b
σ_{fit} (kHz)	4.7		3.2	3.6	3.3	2.5	5.7	3.4
N	42		24	18	27	8	7	9

^a DFT-calculated values, obtained using B3PW91 level/aug cc-pVTZ for C, H, and O and Hay–Wadt VDZ (n+1) ECP for Os. See text for more details.
^b Held fixed to most abundant ^{192}Os values during the fit.

Table 5. Results from the Structural Fit Showing Measured and Calculated Rotational Constants (A, B, C) for Various Isotopomers of $\text{C}_2\text{H}_4\text{Os}(\text{CO})_4$ ^a

isotopomer	parameter	measured	calculated	M–C
^{192}Os	A	929.3256	929.3329	-0.0073
	B	755.1707	755.1739	-0.0032
	C	752.7446	752.7480	-0.0034
^{190}Os	A	929.3328	929.3417	-0.0089
	B	755.1689	755.1739	-0.0050
	C	752.7494	752.7537	-0.0043
^{188}Os	A	929.3407	929.3506	-0.0099
	B	755.1666	755.1739	-0.0073
	C	752.7545	752.7596	-0.0051
$^{13}\text{C}_{\text{equatorial}}$	A	923.1201	923.1013	0.0188
	B	753.9757	753.9358	0.0399
	C	749.8525	749.8751	-0.0226
$^{13}\text{C}_{\text{axial}}$	A	929.2751	929.2652	0.0099
	B	750.9077	750.9127	-0.0050
	C	748.4802	748.4701	0.0101
$^{13}\text{C}_{\text{ethylene}}$	A	920.6996	920.7018	-0.0022
	B	754.9994	754.9983	0.0011
	C	747.2494	747.2472	0.0022
perdeuterated	A	881.4489	881.4493	-0.0004
	B	744.4294	744.4275	0.0019
	C	724.3714	724.3706	0.0008

^a All the values are in megahertz, and the standard deviation of the fit is 15 kHz.

since we have measured multiple Os-substituted isotopomers, the perdeuterated species, and all the unique ^{13}C isotopomers for this molecule. Kraitchman analysis was important because the Kraitchman-derived coordinates are not subject to the same correlation effects present in the least-squares structural fit. Given that the Kraitchman analysis uses the changes in the moments of inertia due to single or multiple (*vide infra*) isotopic substitution, and these moments are related to the squares of

Table 6. Cartesian Atomic Coordinates (Å) in the Principal Axis System Obtained from the Least-Squares Fit to the Measured Rotational Constants for $\text{C}_2\text{H}_4\text{Os}(\text{CO})_4$ ^a

atom	a	b	c	atom	a	b	c
Os	0.000	0.051	0.000	O3	-3.082	0.290	0.000
C2	0.000	-1.123	1.552	C5	0.000	2.141	0.716
C4	0.000	-1.123	-1.552	C6	0.000	2.141	-0.716
O2	0.000	-1.813	2.464	H1	0.893	2.409	1.266
O4	0.000	-1.813	-2.464	H2	-0.893	2.409	1.266
C1	1.948	0.202	0.000	H3	-0.893	2.409	-1.266
C3	-1.948	0.202	0.000	H4	0.893	2.409	-1.266
O1	3.083	0.290	0.000				

^a Uncertainties in the coordinates are estimated to be 0.005 Å.

the coordinates of the substituted atoms, one can only obtain the absolute values of these coordinates. Because the Os atom lies so close to the center of mass (COM), the Kraitchman analysis to obtain the Os coordinates is less reliable, and nonzero $|a|$, $|b|$, and $|c|$ coordinates with significant uncertainties were obtained. However, from symmetry considerations, the Os atom must lie on the b principal axis (Figure 1), with both $|a|$ and $|c| = 0$, and we have assumed these values in the analysis. We then used the absolute distance of the substituted Os atom from the COM as the Os $|b|$ coordinate. The absolute distance from the COM is a simple function of the changes in the moments of inertia upon isotopic substitution and can be determined more precisely than the individual components.

(c) **Tetracarbonylethyleneosmium- d_4 , $\text{Os}(\text{CO})_4(\eta^2\text{-C}_2\text{D}_4)$.** Changes in the moments of inertia for quadruple substitution of the four equivalent hydrogen atoms in $\text{Fe}(\text{CO})_4(\eta^2\text{-C}_2\text{H}_4)$ were considered in an earlier paper.²⁴ The equations are reviewed briefly here, since the principal axes are different for $\text{Os}(\text{CO})_4(\eta^2\text{-C}_2\text{H}_4)$. The basic equation for single isotopic substitution,

Table 7. Comparison of Present Microwave Structural Parameters Obtained for $C_2H_4Os(CO)_4$ with Those Obtained by X-ray and DFT Analysis, the Analogous $C_2H_4Fe(CO)_4$ Molecule, and the Closely Related Species, $H_2Os(CO)_4$ ^a

parameter	$C_2H_4Os(CO)_4$				$C_2H_4Fe(CO)_4$	$H_2Os(CO)_4$
	microwave (structural fit)	microwave (Kraitchman)	X-ray ^b	DFT	microwave ^c	microwave ^d
M–C _{ax}	1.954(2)	1.951	1.943(17)	1.955	1.815(2)	1.958(12)
M–C _{eq}	1.946(5)	1.944	1.920(12)	1.938	1.806(9)	1.968(16)
M–C _{et}	2.209(5)	2.204	2.221(10)	2.223	2.117(14)	1.720(11) ^f
C _{et} –H _{et}	1.083 ^e	1.085		1.083	1.070(4)	
C _{et} –C _{et}	1.432(5)	1.426	1.488(24)	1.434	1.421(7)	
C _{ax} –O _{ax}	1.138 ^e		1.139(20)	1.138	1.142(3)	1.130 ^e
C _{eq} –O _{eq}	1.144 ^e		1.145(15)	1.144	1.145(3)	1.143 ^e
∠C _{eq} MC _{eq}	105.8(3)	103.7	106.0(7)	105.3	111.7(9)	99.0(20)
∠C _{ax} MC _{ax}	171.1(9)	173.3	171.3(5)	172.8	174.9(22)	163.0(30)
∠C _{et} MC _{et}	37.8(2)	37.5	39.2(6)	38.0	39.2(5)	88.3(7) ^g
∠C _{et} C _{et} H _{et}	120.3(1)	120.7		119.0	120.6(5)	
∠H _{et} C _{et} H _{et}	111.2(1)	111.0		113.0	113.6(5)	
∠CH ₂ –C–C (∠out of plane)	26.0(3)	25.9		27.8	21.8(1)	

^a “M” denotes the respective metal atom, Os or Fe, for each complex. Here, bond lengths are in angstroms and bond angles are in degrees. The listed errors are 2σ or larger for parameters with significant correlation. ^b Reference 19. ^c Reference 24. ^d Reference 25. ^e Held fixed to DFT during the fit. ^f Os–H bond distance. ^g ∠HOsH interbond angle for the Os(CO)₄H₂ complex. Estimated errors for Kraitchman analysis are ± 0.01 Å for bond lengths and $\pm 2^\circ$ for bond angles.

given below as eq 1 (also eq 13.35 of ref 41), can be used, as long as the magnitudes of the coordinates in the parent principal axis system are the same for all substituted atoms:

$$\Delta I_{aa} = \Delta m(b_s^2 + c_s^2) - \frac{(\sum_i^N \Delta m b_{si})^2}{M + \Delta m} - \frac{(\sum_i^N \Delta m c_{si})^2}{M + \Delta m} \quad (1)$$

where Δm is the difference between the total mass of the parent (M) and the substituted isotopomer, the subscript “s” refers to the coordinates of the substituted atom(s), and the second and third terms account for the shift of the center of mass from the parent molecule. The analogous terms for ΔI_{bb} and ΔI_{cc} can be obtained by cyclic permutation of the a, b, c coordinates in eq 1. For substitution on a single atom, the second and third terms are typically combined with their corresponding substitution coordinate to give a single term involving the substitution reduced mass, $\mu = \Delta m M / (\Delta m + M)$. For multiple substitution cases where the initial symmetry of the parent is retained, one or both of the last two terms in eq 1 may be zero. For tetracarbonyl ethylene osmium, there are ab and bc mirror planes associated with the C_{2v} symmetry of the complex. The plane containing the ethylene hydrogen atoms is perpendicular to the c -axis, so the quadruple D substitution will only cause a change in the c coordinate of the center of mass; thus, all second and third terms in eq 1 for ΔI_{aa} , ΔI_{bb} , and ΔI_{cc} will be zero except for those containing the b_i coordinates. The second term in eq 1 for ΔI_{aa} and ΔI_{cc} remains and, when combined with $\Delta m b_s^2$, can be shown to reduce to μ . Therefore, the difference moments for quadruple deuterium substitution in this molecule can be simplified and expressed as

$$\Delta I_{aa} = \Delta m c_H^2 + \mu b_H^2, \quad \Delta I_{bb} = \Delta m (a_H^2 + c_H^2), \\ \Delta I_{cc} = \Delta m a_H^2 + \mu b_H^2; \quad \Delta m = 4(m_D - m_H) \quad (2)$$

Since the quadruple substitution does not rotate the principal axes, there are no off-diagonal terms in the inertial tensor for the substituted molecule. This allows for rapid solution of the three difference moments in eq 2 to give the hydrogen substitution coordinates,

$$|a| = \sqrt{\frac{\Delta I_{bb} + \Delta I_{cc} - \Delta I_{aa}}{2\Delta m}}, \quad |b| = \sqrt{\frac{\Delta I_{cc} + \Delta I_{aa} - \Delta I_{bb}}{2\Delta \mu}}, \\ |c| = \sqrt{\frac{\Delta I_{aa} + \Delta I_{bb} - \Delta I_{cc}}{2\Delta m}} \quad (3)$$

These equations were used to determine a_s , b_s , and c_s for the hydrogen atoms.

The coordinates determined in the parent-molecule ($^{192}Os(CO)_4C_2H_4$) principal axis system are presented in Table 8, along with the absolute distance to the COM for each atom. The various molecular structure parameters derived from the Kraitchman analysis coordinates are given in Table 7, along with the respective values obtained from the least-squares structural fit. The estimated errors from Kraitchman analyses are ± 0.01 Å for atom coordinates and bond lengths and $\pm 2^\circ$ for bond angles.

VI. Discussion

Microwave spectroscopy measurements for seven unique tetracarbonyl ethylene osmium isotopomers have yielded the first accurate gas-phase structural parameters for this complex. The structural data obtained by the various methods (least-squares, Kraitchman, and DFT from the present work, and the previous X-ray¹⁹) are summarized in Table 7. We first note the excellent agreement between the parameters obtained by Kraitchman analysis and the least-squares structural fit and, furthermore, the accuracy with which our best DFT method reproduces the experimental structure. The Kraitchman-determined experimental value for the C_{et}–H bond distance (1.085 Å) illustrates that fixing this parameter to the DFT value (1.083 Å) does not cause significant error in the structure-fit analysis. However, the effective (r_0) C–H bond would be expected to be slightly (~ 0.01 Å) longer than both the DFT (r_e) and Kraitchman (r_s) values due to vibrational averaging effects. As noted above, the derived Kraitchman values for the $r(OsC_{ax})$ and $r(OsC_{eq})$ bond distances confirm the corresponding structure-fit parameters, which were found to be correlated. Furthermore, these data confirm the general trend among the X-ray,¹⁹ DFT, and $Fe(CO)_4(\eta^2-C_2H_4)$ ²⁴ microwave results that the M–C_{ax} distance is slightly longer than the M–C_{eq} distance. The agreement

Table 8. Results Obtained from Kraitchman Analysis Showing Absolute Values of Substituted Atomic Coordinates in the Parent ($^{192}\text{Os}(\text{CO})_4\text{C}_2\text{H}_4$) Principal Axis System

atom	$ a_s $ (Å)	$ b_s $ (Å)	$ c_s $ (Å)	r_{com} (Å)
Os	0.000	0.051	0.000	0.051
C _{ax}	1.948	0.169	0.000	1.955
C _{eq}	0.000	1.146	1.529	1.911
C _{et}	0.000	2.141	0.713	2.256
H _{et} ^a	0.894	2.409	1.267	2.409

^a Values derived from quadruple substitution of hydrogen.

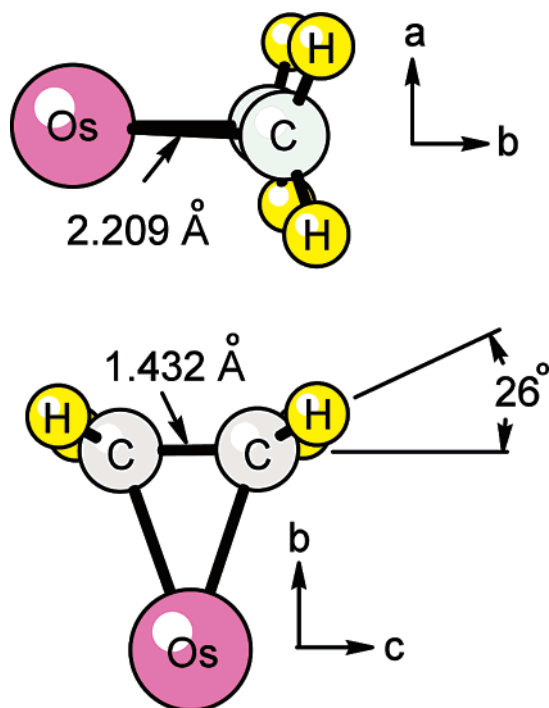


Figure 3. Osmium-ethylene fragment of the molecule, showing some key bond lengths and interbond angles. The lower figure illustrates the angle between the extended carbon-carbon bond and the plane of CH_2 (\angle out of plane).

between the Kraitchman and structure-fit $\text{C}_{\text{ax}}\text{OsC}_{\text{ax}}$ and $\text{C}_{\text{eq}}\text{OsC}_{\text{eq}}$ angles is not as good, but it is satisfactory. The experimental $r(\text{Os}-\text{C}_{\text{et}})$ distance is slightly shorter than values obtained by X-ray diffraction and DFT predictions.

The important and most interesting result is the large and significant deformation of the ethylene ligand upon coordination to the osmium atom. We have obtained an ethylene C-C bond length of 1.43 Å, which falls between the free ethylene average $r_{\text{c}}(\text{C}=\text{C})$ value⁴² of 1.3391(13) Å and the $r_0(\text{C}-\text{C})$ bond length⁴³ of 1.534(2) Å for ethane. Furthermore, the angle between the plane of the CH_2 group and the extended C-C bond (\angle out-of-plane) is 26° . This correlates with the $\angle\text{Os}-\text{C}-\text{C}-\text{H}$ dihedral (torsional) angle of 106.7° , again halfway between the 90° expected for unperturbed ethylene and the 120° expected for pure sp^3 -hybridized carbon atoms. Finally, the observed $\text{HC}_{\text{et}}\text{H}$ angle is 111° , further supporting the metallacyclopropane nature of the complex. Figure 3 illustrates the structure-fit bond lengths and interbond angles obtained for the osmium-ethylene fragment.

The main discrepancy between the gas-phase structure and the previously reported X-ray structure¹⁹ is the ethylene C-C

bond length. The present value of 1.43 Å is in much better agreement with all the available theoretical calculations.^{19,22,23} In the X-ray study, the authors placed the hydrogen atoms in idealized positions, with a C-H bond length of 0.96 Å. It is also likely that the degree of distortion of the C-H bonds out of the ethylene plane was underestimated in the X-ray work. These constraints possibly led to the longer than expected C-C bond length (1.488(24) Å), with a relatively large uncertainty. Norton and co-workers²¹ also reported an angle between the plane of the CH_2 group and the extended C-C bond (\angle out-of-plane) of $31.27(2)^\circ$ from solution-phase ^1H NMR measurements taken in liquid crystal solvents. This value, while a bit large, appears to be a reasonable result, considering that their method could only give the relative size and approximate shape of the ethylene group and that the authors used the dubious X-ray C-C bond length (1.488(24) Å) as the scale factor to get the absolute geometry.

Comparing the present $\text{Os}(\text{CO})_4(\text{C}_2\text{H}_4)$ gas-phase structure with that of $\text{Fe}(\text{CO})_4(\text{C}_2\text{H}_4)$ obtained from FTMW measurements,²⁴ we conclude that the degree of metal(d_{π}) \rightarrow olefin(π^*) back-bonding is somewhat greater for the Os complex, so the changes in the complexed ethylene structure are greater. In the Os complex, the bending of the CH_2 group from the ethylene plane is $26.0(3)^\circ$ versus $21.8(1)^\circ$ for the Fe species. The osmium $\text{H}_{\text{et}}\text{C}_{\text{et}}\text{H}_{\text{et}}$ angle ($111.2(1)^\circ$) is slightly closer to the sp^3 angle than in the iron complex ($113.6(5)^\circ$), and the C-C bond is slightly shorter for the iron complex (1.421(7) versus 1.432(5) Å). This is in agreement with previous DFT studies of the ethylene carbonyl complexes of the d^8 metals.^{22,23} Li et al.²² have pointed out that the relativistic contraction of the 6s orbital for Os decreases the effective nuclear charge felt by the 5d atomic orbitals, causing them to destabilize and expand. This destabilization increases the metal $d(\sigma)$ -olefin π energy gap and decreases the σ -bonding orbital overlap (see Figure 5 of ref 22). However, the $d(\pi)$ -olefin π^* energy gap becomes smaller, thus increasing metal \rightarrow olefin back-bonding.

When the ethylene ligand is replaced by two hydride ligands in $\text{H}_2\text{Os}(\text{CO})_4$,²⁵ significant changes in the $\text{C}_{\text{eq}}\text{OsC}_{\text{eq}}$ and $\text{C}_{\text{ax}}\text{OsC}_{\text{ax}}$ angles occur (Table 7). The hydride ligands reside in the equatorial plane with an H-Os-H angle of $88.3(7)^\circ$. The $\text{H}_2\text{Os}(\text{CO})_4$ complex is thus “pseudo-octahedral”, and it is not surprising that the $\text{C}_{\text{eq}}\text{OsC}_{\text{eq}}$ angle ($99(2)^\circ$) is smaller than in the nearly trigonal bipyramidal $\text{Os}(\text{CO})_4(\text{C}_2\text{H}_4)$ complex ($105.8(3)^\circ$). However, the axial carbonyl ligands tilt even further toward the hydride ligands, with $\angle\text{C}_{\text{ax}}\text{OsC}_{\text{ax}} = 163(3)^\circ$. The reason for the tilt of the axial carbonyls toward any ligands which are less effective π acceptors than CO has been discussed in detail by Bender and Norton et al.¹⁹ and will not be repeated here. We note that their analysis implied a greater back-bonding from the metal to the equatorial carbonyls than to the axial ones, resulting in shorter $\text{M}-\text{C}_{\text{eq}}$ bonds. This trend is confirmed in both the $\text{Os}(\text{CO})_4(\text{C}_2\text{H}_4)$ and $\text{Fe}(\text{CO})_4(\text{C}_2\text{H}_4)$ structures, but the larger uncertainty in the $r(\text{OsC}_{\text{ax}})$ and $r(\text{OsC}_{\text{eq}})$ bond distances in the $\text{H}_2\text{Os}(\text{CO})_4$ structure prevents a reliable comparison.

VII. Conclusions

In the present work, we have obtained the first nearly complete, gas-phase structure of the $\text{Os}(\text{CO})_4(\eta^2\text{-C}_2\text{H}_4)$ complex, including accurate and precise ethylene carbon and hydrogen atom coordinates. The structural parameters determined from

(42) Hirota, E.; Endo, Y.; Saito, S.; Yoshida, K.; Yamaguchi, I. *J. Mol. Spectrosc.* **1981**, *89*, 223.

(43) Shaw, D. E.; Lepard, D. W.; Welsh, H. L. *J. Chem. Phys.* **1965**, *42*, 3736.

Kraitchman analysis and least-squares structural fit are in excellent agreement with those obtained from density functional theory calculations and indicate a substantial rehybridization of the ethylene carbons upon coordination to the osmium atom. The ethylene C–C bond length is elongated by 0.09 Å relative to that in free ethylene, and the angle between the plane of the CH₂ group and the C–C bond is 26.0(3)°. We also find that the degree of metal → olefin back-bonding of the osmium complex is greater than in the analogous Fe(CO)₄(C₂H₄) complex. These results confirm the statement of Norton and co-workers^{19–21} that tetracarbonylethyleneosmium is closer to a metallacyclopropane than to a simple π-complex.

Acknowledgment. We thank Prof. Josef Takats, University of Alberta, for his continued help and support on this project. He has generously provided much essential advice and unique laboratory facilities for conducting the Os(CO)₅ chemistry and

many helpful comments on the manuscript. Acknowledgment is made to the donors of The American Chemical Society Petroleum Research Fund for partial support of this research. This material is based, in part, upon work supported by the National Science Foundation under Grant 0304969. We are very grateful for the support from these agencies. We are extremely grateful to Giles L. Henderson and Richard Keiter of Eastern Illinois University for originating this spectroscopy project in 1992.

Supporting Information Available: Complete ref 35; figure showing the construction of the photochemical immersion well. This information is available free of charge via the Internet at <http://pubs.acs.org>.

JA0727969